Journal of
Ceramic Science
and Technology

J. Ceram. Sci. Tech., **04** [02] 105-112 (2013)
DOI: 10.4416/JCST2012-00041
available online at: http://www.ceramic-science.com

Characterisation of SiCN Coatings on Substrates of Hf and Nb

C. Delpero*, W. Krenkel, G. Motz

University of Bayreuth, Ceramic Materials Engineering (CME), D-95440 Bayreuth, Germany
received October 1, 2012; received in revised form November 23, 2012; accepted January 21, 2013

Abstract

Refractory metals like Hf and Nb have high hardness and melting points above 2000 °C which make them attractive candidates for high-temperature applications. In this work it was investigated whether these metals can be used as a basis for the development of metal-ceramic composite materials. Because of the tendency of the metals to form carbide and nitride phases, a preceramic SiCN-precursor was chosen for the synthesis of the ceramic coating. During pyrolysis a functionally graded intermediate layer consisting of metal carbide and nitride is formed by reaction with the precursor elements, which also depends on the pyrolysis atmosphere used. Previous work indicates that the adhesion between the precursor-derived ceramic coating and the metal is improved if such a layer is formed [1,2]. In this work functionally graded layers were synthesised on substrates of hafnium and niobium using the polymer ABSE for the reactive precursor coating and nitrogen respectively argon as the pyrolysis atmosphere. The resulting layer systems were characterised by means of glow discharge optical emission spectroscopy, X-ray diffraction, electron microprobe analysis, scanning electron microscopy and transmission electron microscopy.

Keywords: Precursor-derived ceramics, FGM, transition metals, composites, SiCN

I. Introduction

Precursor ceramic technology has been intensively researched in recent decades. Starting with the synthesis of phosphorous nitride from phosphorous nitride chloride [3] and SiO_2 from siloxanes [4] a wide range of preceramic polymers for the synthesis of ceramics has been investigated. The work of Yajima *et al.* in the 1970s on non-oxide silicon-based ceramics hasbeen the biggest influence on the rising interest in preceramic polymers [5,6]. Owing to the shrinking of the precursor during pyrolysis, precursor-derived ceramics (PDCs) have been limited to low-dimensional applications such as fibres [7,8], thin films [9,10] or as binder material in ceramic powders [11,12]. In order to compensate for the volume change during the polymer-ceramic conversion, Greil *et al.* have developed the AFCOP (active-filler-controlled pyrolysis) process [13–15]. Filler materials in the precursor react with the gaseous pyrolysis products and expand their volume to partially or fully compensate for the shrinkage of the ceramic. Typically transition metals like titanium have shown a high affinity for the reaction with the pyrolysis products [16–17].

This precursor route is an alternative approach to the development of quasi ductile composite materials like e.g. CMCs [18–19]. In this work advantage has been taken of the reactivity of the transition metals hafnium and niobium with the precursor elements to synthesise ceramic gradient layers on metal substrates. This was inspired by the development of functionally graded materials (FGMs) [20], which use gradient layers to achieve good adhesion between a ceramic layer and a metallic substrate. There is already some evidence to suggest that an intermediate gradient layer is formed by diffusion of precursor elements into the metal [21–24]. To examine the formation of the gradient layers, substrates of hafnium and niobium were coated with a precursor and pyrolysed with different pyrolysis parameters. Furthermore, the influence of a reactive pyrolysis atmosphere on the formation of the gradient layer was examined. The precursor for these experiments was the ammonolysed bis(dichlormethyl)silylethane polymer (ABSE) which is solid at room temperature and soluble in non-polar solvents. The refractory metals chosen were hafnium and niobium as these metals show a high affinity to forming carbides and nitrides in the presence of carbon and nitrogen.

II. Experimental

The preparation of the ABSE polycarbosilazane is performed by ammonolysis of bis(dichloromethyl)silylethane in toluene, which has already been described in the literature [25,26]. A ceramic yield of 75 % has been determined for the ABSE precursor. The metal sheets of hafnium, niobium and molybdenum were polished with 320 mm SiC paper and 3 μm diamond suspension to reduce the arithmetic average roughness height to 0.1 – 0.2 μm. After they had been polished, the samples were cleaned with acetone in an ultrasonic bath for 15 min. The precursor was applied by dip-coating metal sheets into a 10 % solution of ABSE in toluene with a hoisting speed of 1.94 mm/s to produce a polymer coating of about 1 μm thickness, which yields a ceramic coating of about 0.5 μm after pyrolysis [23]. After they had been coated, the samples were pyrolysed at 800, 1000 or 1300 °C with a heating

* Corresponding author: Email: christian@delpero.de

rate of 3 K/min to analyse the temperature dependence of the gradient layer formation. The minimum temperature required to achieve complete ceramization of the ABSE polymer is 800 °C. Also, diffusion rates below 800 °C have proven to be too low to produce any significant gradient layer. 1300 °C was chosen as the highest pyrolysis temperature as the ceramic layer already becomes very thin at this temperature because all precursor elements start diffusing into the substrate at this temperature [27]. Argon was used as an inert gas for pyrolysis, while N_2 gas ($O_2 < 50$ vpm) with a flow rate of 200 ml/min was used as a reactive atmosphere to provide additional nitrogen for the formation of the gradient layer. To investigate the time dependence, the samples were pyrolysed at 1000 °C for 1, 10 or 100 h.

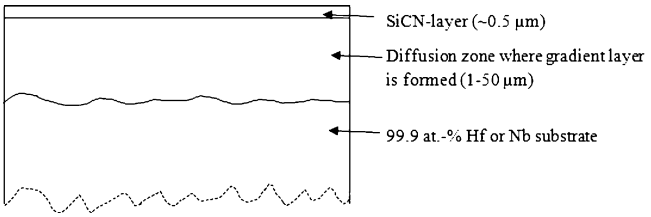

Fig. 1: Schematic showing a cross-section of coated and pyrolysed sample.

Fig. 1 shows the schematic model of the cross-section of a coated and pyrolysed sample. After pyrolysis the SiCN-layer has a thickness of about 0.5 μm, the diffusion zone is between 1 to 50 μm depending on the pyrolysis parameters.

After pyrolysis, nitride and carbide phases were identified with X-ray diffraction analysis (Seifert ID 3000, CuK_α). Depth profiling of the gradient layers was performed via glow discharge optical emission spectroscopy (Spectruma GDA 750). Cross-sections of the samples were prepared both by metallographic methods and with focused ion beam etching. The cross-sections were examined with scanning electron microscopy (Carl Zeiss 1540EsB Cross Beam) and transmission electron microscopy (Carl Zeiss Libra 200 FE). The Carl Zeiss 1540EsB Cross Beam is based on cross beam technology and can use both electron and ion beams. The chemical composition of the cross-sections was determined with a JEOL JXA-8200 electron microprobe.

III. Results and Discussion

(1) Thermogravimetric analysis

In a preliminary experiment the affinity of the metals to reacting with nitrogen was examined with thermal gravimetric analysis (TGA) to see whether the samples would react with gaseous nitrogen. Niobium nitride and hafnium nitride have high formation enthalpies of 326.0 resp. 369.4 kJ/mol, while molybdenum nitride has a very low formation enthalpy of 70.0 kJ/mol. As shown in Fig. 2, both hafnium and niobium show significant mass change at temperatures above 1000 °C under nitrogen. Thus, the thickness of the gradient layers in hafnium and niobium can be increased by choosing nitrogen as the pyrolysis atmosphere. Molybdenum shows no reactivity with gaseous N_2 as shown previously [27]. Therefore, it was not included in further investigations.

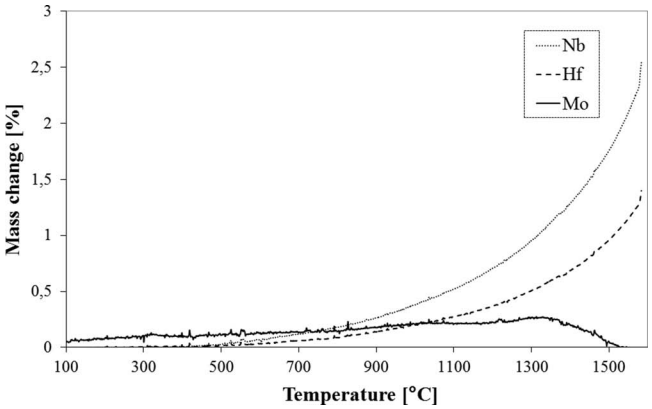

Fig. 2: Thermogravimetric analysis of hafnium, niobium and molybdenum samples under N_2 with a heating rate of 3 K/min.

(2) X-ray diffraction analysis

First, the compositions of the phases that were formed in the gradient layer under different pyrolysis parameters were determined. Most important was the investigation of the influence of temperature and pyrolysis atmosphere on the crystallographic phases formed in the diffusion zone. As the ABSE precursor provides both carbon- and nitrogen-containing gaseous products, it is possible that either carbides, nitrides or a mixture of both phases are formed. The stoichiometric composition of the resulting carbide and nitride phases was also of interest. The phase diagrams of Hf-N, Hf-C, Nb-C and Nb-N give indications of the phases that appear at a certain temperature during pyrolysis. However, the pyrolysis time might not be sufficient to reach thermal equilibrium and thus for all phases that are stable according to the phase diagram to be formed.

With X-ray diffraction analysis (XRD) all crystalline phases present near the surface of the sample can be characterised. As the SiCN-layer is amorphous after annealing at temperatures below 1350 °C it cannot be detected by diffraction methods. The angle-dependent mean penetration depth of the X-ray beam can be calculated from the X-ray attenuation coefficient of the materials. Thus, the information of the X-ray detection comes from a depth of up to 5 – 10 μm in the selected materials, which is sufficient to analyse the composition of the gradient layer.

(a) *Hafnium substrates*

In Fig. 3a the X-ray diffraction signals are shown for three hafnium samples coated with an ABSE layer of 1 μm thickness that have been pyrolysed for 1, 10 and 100 h at 1000 °C under flowing nitrogen. It is evident that the gradient layer is only composed of nitride phases. According to the hafnium-nitrogen phase diagram there are three stable nitride phases at this temperature, namely α-$HfN_{0.4}$, η-Hf_3N_2 and δ-HfN. The XRD measurements show that δ-HfN is only formed after annealing for more than 10 h. Only after 100 h can all three phases that appear in the phase diagram at this temperature be detected. The signal of the pure hafnium phase (α-Hf) vanishes after pyrolysis for 10 h, which indicates that the surface is nitrided at least up to the penetration depth of the CuK_α radiation, which is about 7.5 μm in hafnium at an incidence angle of 50°.

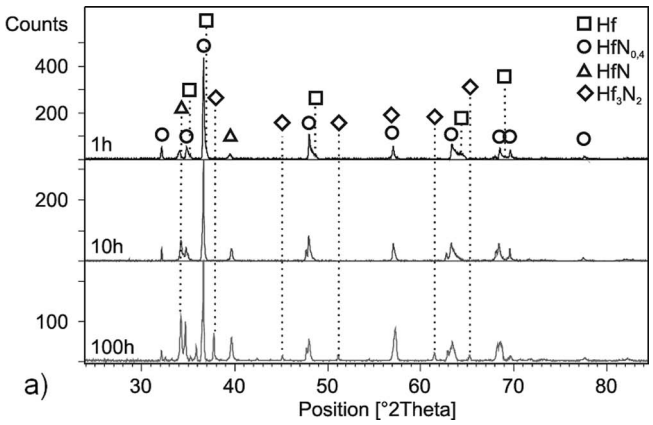

Fig. 3a: X-ray diffraction measurements for ABSE-coated hafnium samples after pyrolysis for 1, 10 and 100 h at 1000 °C under $\mathbf{N_2}$ **atmosphere**.

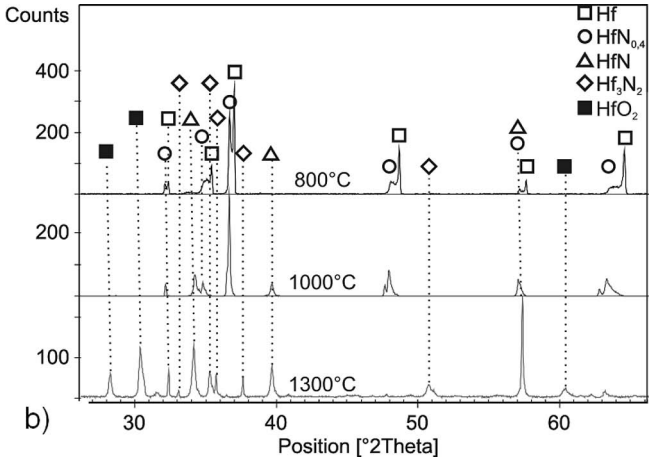

Fig. 3b: X-ray diffraction measurements for ABSE-coated hafnium samples after pyrolysis for 10 h at 800, 1000 and 1300 °C under $\mathbf{N_2}$ **atmosphere**.

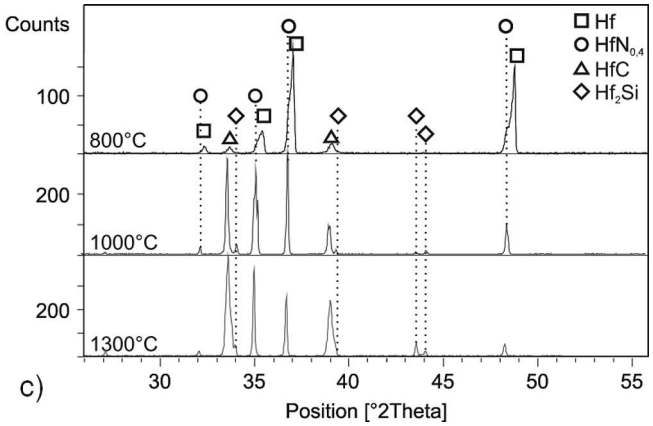

Fig. 3c: X-ray diffraction measurements for ABSE-coated hafnium samples after pyrolysis for 10 h at 800, 1000 and 1300 °C under **Ar atmosphere**.

Fig. 3b shows the phases formed after pyrolysis for 10 h at 800, 1000 and 1300 °C. It can be seen that after pyrolysis at 800 °C the gradient layer consists mostly of $HfN_{0.4}$. The signals of the HfN and Hf_3N_2 phases are not detectable, although these phases should have been formed at this temperature according to the phase diagram of Hf-N [28]. Either these phases have a thickness of only a few 100 nm or they are not formed at all yet. As was observed by Williams *et al.*, a certain transient period transpires after a new phase nucleates at an interface before it begins growing [29]. Because of this, the growth of the HfN and Hf_3N_2 phases might not have begun forming yet after 10 h of pyrolysis. After pyrolysis at 1000 °C the HfN phase can be clearly detected, while the Hf_3N_2 phase still does not appear in the diffraction pattern. After pyrolysis for 10 h at 1300 °C all three hafnium nitride phases that appear in the phase diagram can be found. The signals of Hf and $HfN_{0.4}$ vanish from the diffraction pattern, which indicates that the gradient layer's thickness is greater than the penetration depth of the CuKα radiation in hafnium nitride. The HfN and Hf_3N_2 phases combined now have to exceed a thickness of 7.5 μm, which is also the average penetration depth for CuKα radiation in hafnium.

Fig. 3c shows the results of the X-ray diffraction measurements for ABSE-coated hafnium samples that have been pyrolysed for 10 h at 800, 1000 and 1300 °C under an inert argon atmosphere. Most notable is the formation of hafnium carbide under these conditions at all temperatures. The only hafnium nitride phase formed is $HfN_{0.4}$, which is formed without phase transition. Thus it can be concluded that the primary reaction with the hafnium substrate is with the free carbon that is formed during the pyrolysis of the ABSE precursor. HfC is the only known stable hafnium carbide phase at this temperature [30]. The gaseous nitrogen species formed during the pyrolysis are not sufficient to create HfN or Hf_3N_2. This result shows that the metal primarily reacts with carbon created during pyrolysis and to a lesser extent with the nitrogen in the precursor. If there is a sufficient supply of nitrogen from the atmosphere, the reaction of nitrogen suppresses the formation of carbides, and instead nitride phases are formed. Finally, it must be noted that at 1300 °C a hafnium silicide phase is formed by reaction of the silicon content in the precursor with the hafnium substrate. Therefore, it has to be expected that the precursor layer starts disappearing at this temperature as all of its elements start to diffuse into the substrate.

(b) *Niobium substrates*

It is expected that niobium behaves similarly to hafnium as these elements share their affinity to carbon and nitrogen. As can be seen from Fig. 4a, niobium forms exclusively nitride phases after pyrolysis for 1, 10 and 100 h at 1000 °C under nitrogen atmosphere. The Nb_4N_3 phase can only be detected after 100 h of pyrolysis. This can be compared to the formation of the Hf_3N_2 phase on the hafnium substrate, which also takes significantly longer than 10 h to appear in the gradient layer. Analogous to the hafnium substrate, the carbon formed in the precursor during pyrolysis does not react with the metal under nitrogen atmosphere. The supply of nitrogen suppresses the formation of carbides and only nitride phases can be found in the gradient layer.

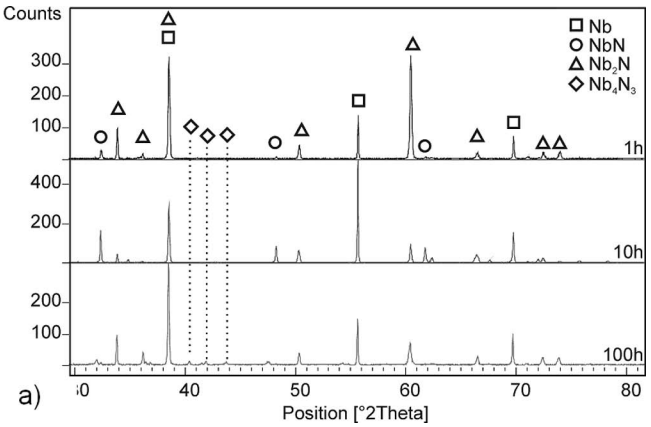

Fig. 4a: X-ray diffraction measurements for ABSE-coated niobium samples after pyrolysis for 1, 10 and 100 h at 1000 °C under $\mathbf{N_2}$ **atmosphere**.

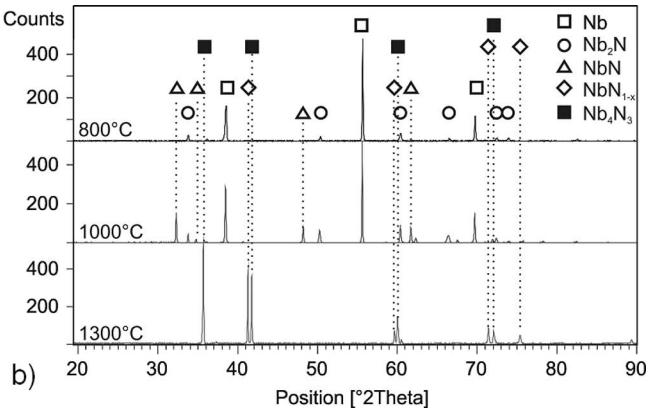

Fig. 4b: X-ray diffraction measurements for ABSE-coated niobium samples after pyrolysis for 10 h at 800, 1000 and 1300 °C under $\mathbf{N_2}$ **atmosphere**.

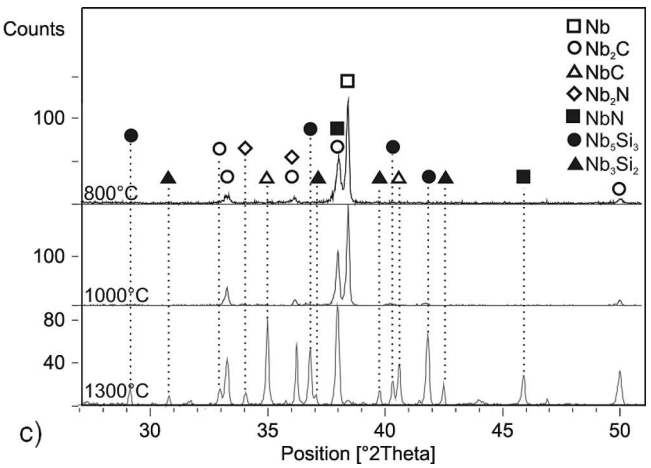

Fig. 4c: X-ray diffraction measurements for ABSE-coated niobium samples after pyrolysis for 10 h at 800, 1000 and 1300 °C under **Ar atmosphere**.

Fig. 4b shows the composition of the gradient layer of an ABSE-coated niobium sample after pyrolysis for 10 h at 800, 1000 and 1300 °C under nitrogen atmosphere. The formation of the Nb_4N_3 phase can be observed after pyrolysis at 1300 °C, while only two different nitride phases (NbN and Nb_2N) are formed at 800 and 1000 °C. Additionally, the phase transition from NbN and Nb_4N_3 to NbN_{1-x} can be observed in the XRD patterns. The Nb_{1-x} phase is formed at temperatures above 1100 °C instead of the NbN and Nb_4N_3 phases [31]. The reason why the Nb_4N_3 phase can still be found after pyrolysis at 1300 °C is that the transformation from the NbN_{1-x} phase to the Nb_4N_3 phase during cooling is a quasi diffusionless process that occurs very fast [30].

Fig. 4c shows the X-ray diffraction patterns of ABSE-coated niobium samples pyrolysed for 10 h at 800, 1000 and 1300 °C under inert argon atmosphere. Just as in the hafnium samples, the formation of carbide phases is favoured over the formation of niobium nitride under an inert atmosphere. After pyrolysis at 1300 °C the Nb_2N phase can be detected, while carbide phases can be found at lower temperatures. Also the silicon from the precursor starts reacting with the niobium substrate at 1300 °C to form silicide phases.

Summarizing these XRD investigations it can be clearly seen that both substrates show comparable results with regard to the formation of the gradient layer. Under nitrogen atmosphere only nitride phases are formed and the reaction of the free carbon in the ABSE precursor is suppressed by the supply of gaseous nitrogen. When an inert atmosphere is used, the main reaction is between the free carbon formed during pyrolysis of the precursor and the metal. Also at 1300 °C the silicon from the ABSE layer starts reacting with both the hafnium and the niobium substrate.

(3) GDOES analysis

In order to analyse the depth-dependent chemical composition of the diffusion zones where the gradient layers are formed, the samples were analysed with glow discharge optical emission spectroscopy (GDOES). With GDOES analysis, the gradient of the different elements in the diffusion zone where the gradient layer is formed can be measured with good depth resolution. The quality of the element quantification depends significantly on the calibration standards used to calibrate the GDOES. Specifically for light elements, like carbon, nitrogen and oxygen, conductive calibration samples with more than 5 – 6 wt% are unavailable, so the results for these concentrations are much less reliable than for values below 5 – 6 wt%.

(a) Hafnium substrates

Fig. 5a shows the result of the GDOES measurement of an ABSE-coated hafnium sample pyrolysed for 10 h at 800 °C under nitrogen atmosphere. It can be seen that both nitrogen and carbon are diffusing into the gradient layer. The thickness of the SiCN-layer was estimated by determining at which value the silicon concentration has dropped to 50 % ($Si_{50\%}$) of the maximum concentration Si_{max}.

The elemental analysis of an ABSE-coated hafnium sample after pyrolysis for 10 h at 1000 °C under nitrogen atmosphere is shown in Fig. 5b. The diffusion zone consists almost entirely of nitrogen and hafnium, which correlates with the XRD measurements, in which only hafnium nitrides were found. This is even more evident for the sample pyrolysed at 1300 °C (see Fig. 5c).

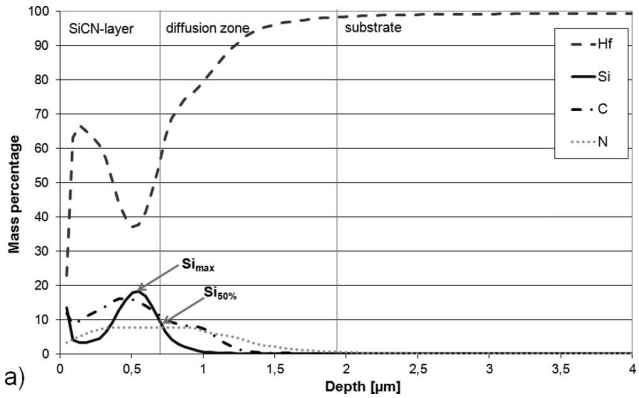

Fig. 5a: GDOES measurement for ABSE-coated hafnium sample after pyrolysis for 10 h at 800 °C under N_2 **atmosphere**.

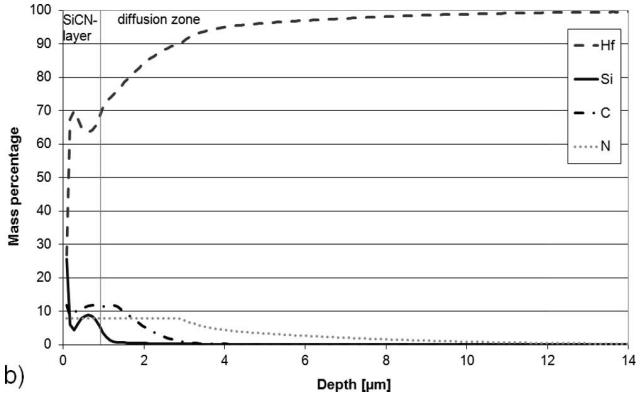

Fig. 5b: GDOES measurement for ABSE-coated hafnium sample after pyrolysis for 10 h at 1000 °C under N_2 **atmosphere**.

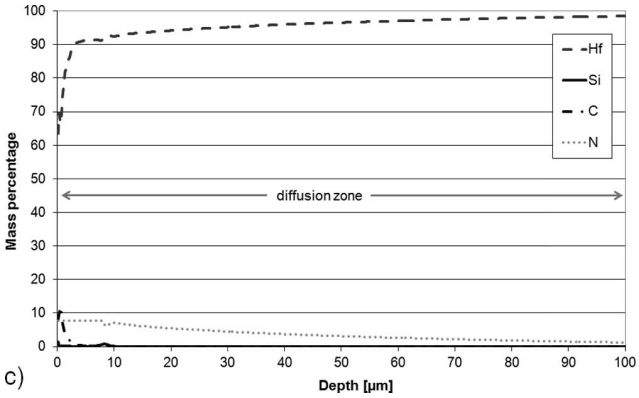

Fig. 5c: GDOES measurement for ABSE-coated hafnium sample after pyrolysis for 10 h at 1300 °C under N_2 **atmosphere**.

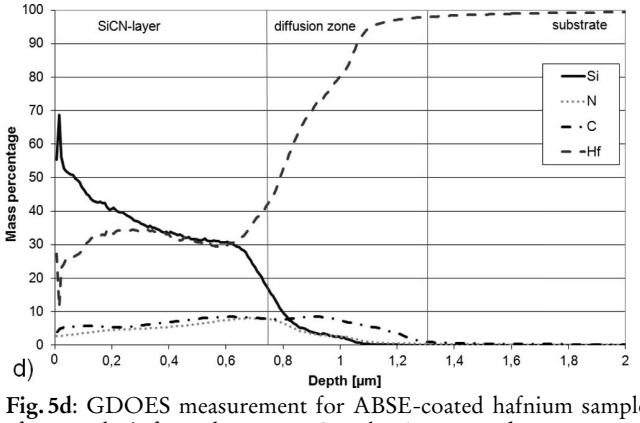

Fig. 5d: GDOES measurement for ABSE-coated hafnium sample after pyrolysis for 10 h at 1000 °C under **Ar atmosphere**.

When the hafnium sample is pyrolysed under an inert argon atmosphere the diffusion layer is much thinner as it is now only composed of the species in the precursor that react with the substrate. Fig. 5d shows the result of the GDOES analysis of a coated sample after pyrolysis for 10 h at 1000 °C under argon atmosphere. In this sample the concentration of carbon in the gradient layer is much higher than the concentration of nitrogen. As expected, the main reaction between the precursor and the metal substrate is due to the diffusion of free carbon formed in the precursor during its transformation from the polymer to the ceramic state.

(b) Niobium substrates

The niobium samples have been pyrolysed with the same parameters as the hafnium samples discussed in the previous section. The niobium samples pyrolysed for 10 h at 1000 resp. 1300 °C under nitrogen atmosphere show that the gradient layer is formed primarily by diffusion of nitrogen into the niobium substrates (Figs. 6a and 6b). Almost no carbon can be detected in the diffusion zone, which is in accordance with the XRD measurements, where only nitride phases were found in these samples.

The reaction between the precursor and the metal also shows similarities to the hafnium substrates. Only carbon is found in the gradient layer after pyrolysis under inert argon atmosphere for 10 h at 1000 °C (Fig. 6c), which confirms the XRD measurements, in which only carbide phases were found in this sample.

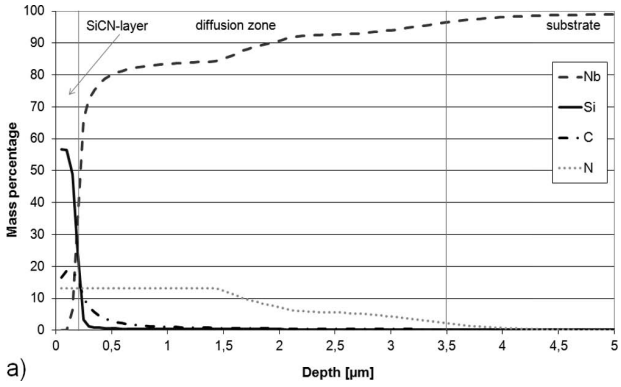

Fig. 6a: GDOES measurement for ABSE-coated niobium sample after pyrolysis for 10 h at 1000 °C under N_2 **atmosphere**.

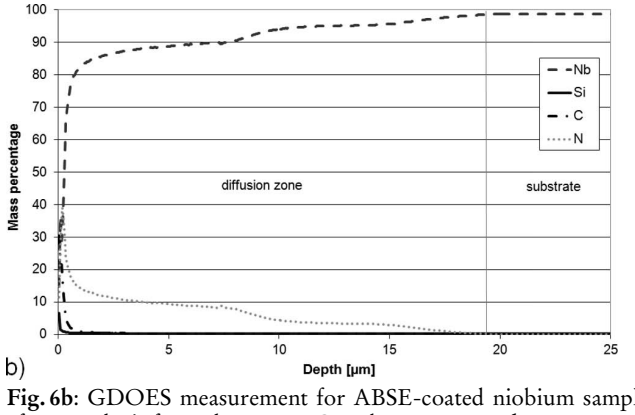

Fig. 6b: GDOES measurement for ABSE-coated niobium sample after pyrolysis for 10 h at 1300 °C under N_2 **atmosphere**.

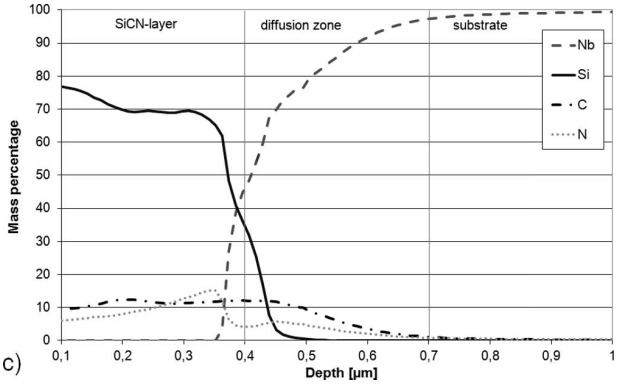

c)

Fig. 6c: GDOES measurement for ABSE-coated niobium sample after pyrolysis for 10 h at 1000 °C under **Ar atmosphere**.

(4) Electron microscopy

(a) *Scanning electron microscopy*

To examine the diffusion zone with scanning electron microscopy, a cross-section through the surface was prepared by etching the sample with a focused ion beam (FIB). The composition within the diffusion zone was imaged with the back scatter electron (BSE) detector. Fig. 7 shows the BSE image of a cross-section through an ABSE-coated niobium sample pyrolysed for 10 h at 1300 °C under nitrogen atmosphere. The two different phases NbN and Nb_2N can be distinguished very well. Analysis with energy-dispersive X-ray analysis (EDX) point measurements confirmed that the two phases found in the diffusion zone are NbN_{1-x} and Nb_2N.

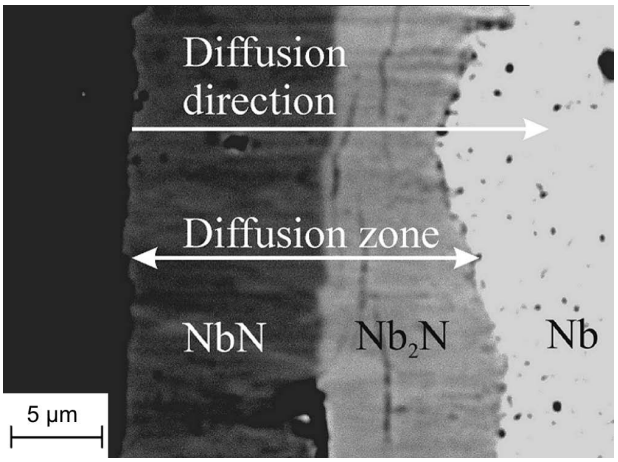

Fig. 7: Back scatter image of cross-section through an ABSE-coated niobium sample after pyrolysis for 10 h at 1300 °C under N_2 atmosphere.

(b) *Electron probe micro-analysis*

In order to characterise the chemical composition of the cross-section more accurately, electron probe micro-analysis (EPMA) was used. EPMA combines wavelength-dispersive X-ray analysis (WDX) with energy-dispersive X-ray analysis for a much higher accuracy than can be obtained with EDX alone. Fig. 8 shows the nitrogen content in the gradient layer of a niobium sample pyrolysed for 10 h at 1300 °C under nitrogen atmosphere. The weight percentages correlate with the composition of the Nb_{1-x} phase (47 – 42 wt%) and the Nb_2N phase (35 – 31 wt%) given in the Nb-N phase diagram.

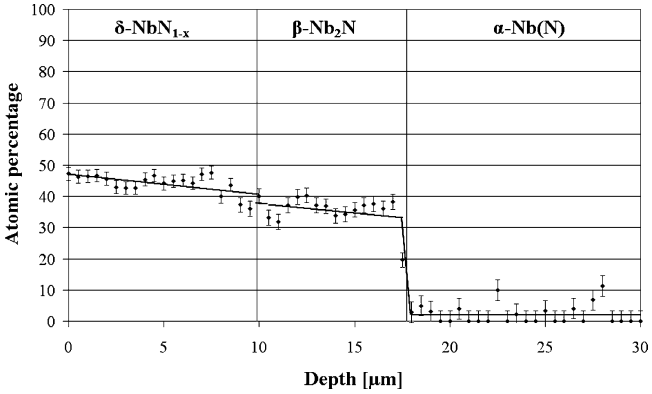

Fig. 8: Electron microprobe analysis of the nitrogen content in the diffusion zone of an ABSE-coated niobium sample after pyrolysis for 10 h at 1300 °C under N_2 atmosphere.

(c) *Transmission electron microscopy*

A thin cross-section of an ABSE-coated niobium sample pyrolysed for 10 h at 1000 °C under nitrogen atmosphere was created with the focused ion beam technique to be analysed in a transmission electron microscope. The different phases in the gradient layer can be seen in a scanning transmission electron microscope image (Fig. 9). By using electron diffraction the phases can be clearly identified. Five electron diffraction patterns were made of each phase (Fig. 10) and indexed using the program JEMS [32]. The phases present in the diffusion zone, NbN, Nb_4N_3 and Nb_2N, are in accordance with the composition of the Nb-N phase diagram at 1000 °C.

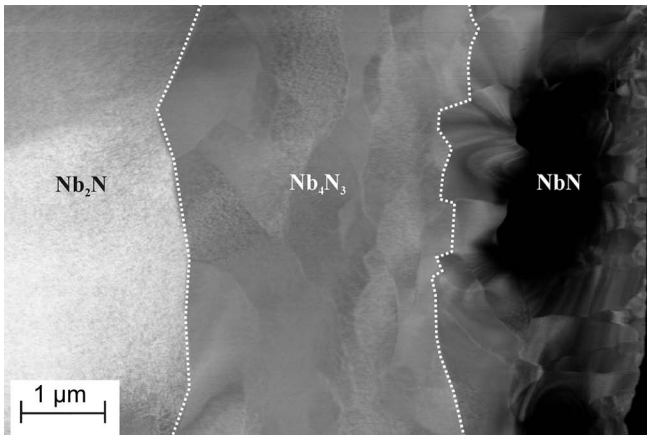

Fig. 9: STEM picture of the diffusion zone in a niobium sample after pyrolysis for 10 h at 1000 °C under N_2 atmosphere.

IV. Conclusions

Gradient layers consisting of nitrides and carbides have been synthesised on transition metal substrates via reactive precursor coating. The pyrolysis temperature has been varied between 800, 1000 and 1300 °C, the pyrolysis time between 1, 10 and 100 h, and the atmosphere altered between flowing nitrogen and argon. The layers were characterised by means of X-ray diffraction, glow discharge optical emission spectroscopy, scanning electron microscopy, transmission electron microscopy and electron microprobe analysis. The influencing parameters such as time, temperature and pyrolysis atmosphere have been investigated.

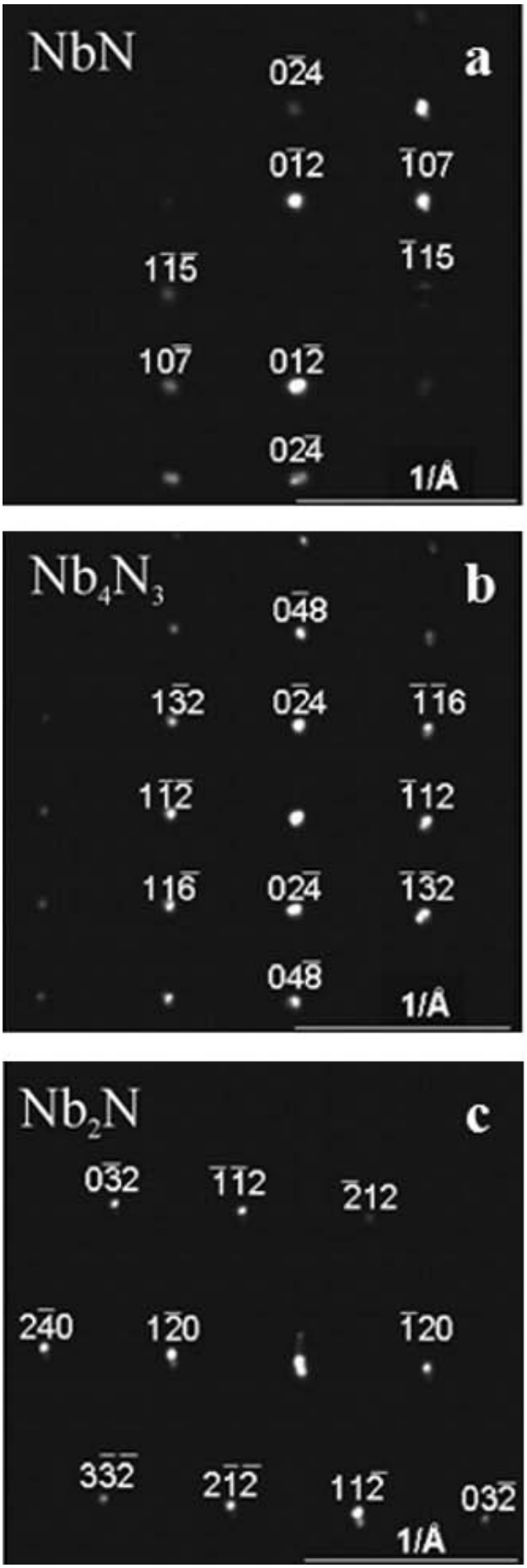

Fig. 10: TEM electron diffraction patterns of the different nitride phases NbN (a), Nb_4N_3 (b) and Nb_2N (c) present in a niobium sample after pyrolysis for 10 h at 1000 °C under N_2 atmosphere.

A gradient layer consisting of nitrides on hafnium and niobium could be synthesised at all three temperatures under nitrogen. The nitrogen from the atmosphere proved to be the primary factor for the development of the gradient layer. Under argon atmosphere the gradient layer was composed of carbides owing to diffusion of carbon from the SiCN-layer into the metal. As the supply of carbon was limited to the carbon source in the precursor coating, these layers were significantly thinner than the gradient layers obtained under a reactive nitrogen atmosphere. At 1300 °C, silicon from the SiCN-layer reacts with the metal to form silicides, thus reducing the thickness of the ceramic layer.

Acknowledgements

We thank the Deutsche Forschungsgemeinschaft (DFG) for financial support of this work. The help of Carl Zeiss in the preparation of the TEM lamella is gratefully acknowledged. The authors express their appreciation to Christian Liebscher at the Chair of Metals and Alloys at the University of Bayreuth for his support in the TEM measurements. We should also like to thank Prof. Stadelmann for providing the program JEMS for the analysis of electron diffraction patterns.

References

1 Torrey, J.D., Bordia, R.K.: Processing of polymer-derived ceramic composite coatings on steel, *J. Am. Ceram. Soc.*, **91**, [1], 41 – 45, (2008).

2 Torrey, J.D., Bordia, R.K.: Mechanical properties of polymer-derived ceramic composite coatings on steel, *J. Eur. Ceram. Soc.*, **28**, [1], 253 – 257, (2007).

3 Aigner, F.W., Herbert, J.M.: The preparation of phosphorous-nitrogen compounds as non porous solids. in: Special Ceramics, P. Popper (ed.), Academic, New York, 1960.

4 Weyer, D. E. (Dow Corning Corp.), US Patent 3090691, 1963.

5 Yajima, S.: SiC sintered bodies with three dimensional polycarbosilane as binder, *Nature*, **264**, 238 – 239, (1976).

6 Yajima, S., Hasegawa, Y., Okamura, K., Matsuzawa, T.: Development of high tensile strength silicon carbide fibre using an organosilicon polymer precursor, *Nature*, **273**, 525 – 527, (1978).

7 Yajima, S., Hayashi, J., Omori, M.: Continuous silicon carbide fiber of high tensile strength, *Chem. Lett.*, 931 – 934, (1975).

8 Yajima, S., Okamura, K., Hayashi, J.: Structural analysis in continuous silicon carbide fiber of high tensile strength, *Chem. Lett.*, 1209 – 1212, (1975).

9 Mucalo, M.R., Milestone, N.B.: Preparation of ceramic coatings from pre-ceramic precursors, part I SiC and "Si_3N_4/Si_2N_2O" coatings on alumina substrates, *J. Mater. Sci.*, **29**, 4487 – 4499, (1994).

10 Mucalo, M.R., Milestone, N.B.: Preparation of ceramic coatings from pre-ceramic precursors, part II SiC on metal substrates, *J. Mater. Sci.*, **29**, 5934 – 5946, (1994).

11 Seyferth, D., Bryson, N., Workman, D.P., Sobon, C.A.: Preceramic polymers as "reagents" in the preparation of ceramics, *J. Am. Ceram. Soc.*, **74**, [10], 2687 – 2689, (1991).

12 Seibold, M., Greil, P.: Thermodynamics and microstructural development of ceramic composite formation by active filler-controlled pyrolysis (AFCOP), *J. Eur. Ceram. Soc.*, **11**, [2], 105 – 113, (1993).

[13] Greil, P., Seibold, M.: Active filler controlled pyrolysis (AFCOP) – A novel fabrication route to ceramic composite materials, *Ceram. Trans.*, **19**, 43 – 49, (1990).

[14] Greil, P., Seibold, M.: Modelling of dimensional changes during polymer-ceramic conversion for bulk component fabrication, *J. Mater. Sci.*, **27**, 1053 – 1060, (1992).

[15] Greil, P.: Active-filler-controlled pyrolysis of preceramic polymers, *J. Am. Ceram. Soc.*, **78**, [4], 835 – 848, (1995).

[16] Torrey, J.D.: Polymer derived ceramic composites as environmental barrier coatings on steel, Dissertation, University of Washington, 2006.

[17] Torrey, J.D., Bordia, R.K., Henager Jr, C.H., Blum, Y., Shin, Y., Samuels, W.D.: Composite polymer derived ceramic system for oxidizing environments, *J. Mater. Sci.*, **41**, 4617 – 4622, (2006).

[18] Krenkel, W., Naslain, R., Schneider, H. (eds.): High temperature ceramic matrix composites, Wiley-VCH, Weinheim (2006)

[19] Krenkel, W.: Carbon fiber reinforced CMC for high-performance structures, *Int. J. Appl. Ceram. Technol.*, **1**, [2], 188 – 200, (2004).

[20] Miyamoto, Y., Kaysser, W.A., Rabin, B.H., Kawasaki, A., Ford, R.G.: Functionally graded materials: Design, Processing and Applications, Materials Technology series, 5, Kluwer Academic Publishers, Dordrecht, Boston, London, 1999

[21] Ryu, H.-Y., Raj, R.: Selection of TiN as the interconnect material for measuring the electrical conductivity of polymer-derived SiCN at high temperatures, *J. Am. Ceram. Soc.*, **90**, [1], 295 – 297, (2007).

[22] Günthner, M., Kraus, T., Dierdorf, A., Decker, D., Krenkel, W., Motz, G.: Particle-filled PHPS silazane-based coatings on steel, *Int. J. Appl. Ceram. Technol.*, **6**, [3], 373 – 380, (2009).

[23] Günthner, M., Kraus, T., Dierdorf, A., Decker, D., Krenkel, W., Motz, G.: Advanced coatings on the basis of Si(C)N precursors for protection of steel against oxidation, *J. Eur. Ceram. Soc.*, **29**, 2061 – 2068, (2009).

[24] Kraus, T., Günthner, M., Krenkel, W., Motz, G.: cBN-particle-filled SiCN-precursor coatings, *Adv. Appl. Ceram.: Struct. Funct. Bioceram.*, **108**, [8], 476 – 482, (2009).

[25] Motz, G., Hacker, J., Ziegler, G.: Special modified silazanes for coatings, fibers and CMC's, 24th Annual Conference on Composites, Advanced Ceramics, Materials, and Structures: B, 21, 307 – 314, (2000).

[26] Trassl, S., Suttor, D., Motz, G., Rössler, E., Ziegler, G.: Structural characterization of silicon carbonitride ceramics derived from polymeric precursors, *J. Eur. Ceram. Soc.*, **20**, 215 – 225, (2000).

[27] Delpero, C., Krenkel, W., Motz, M.: Generation of ceramic layers on transition metals via reaction with SiCN-precursors. In: Advances in Polymer Derived Ceramics and Composites, P. Colombo, R. Raj, M. Singh (eds.), John Wiley & Sons, Inc., Hoboken, NJ, 73 – 79, 2010.

[28] Okamoto, H., The Hf-N (hafnium-nitrogen) system, *J. Phase Equil.*, **11**, [2], 146 – 149, (1990).

[29] Williams, D.S., Rapp, R.A., Hirth, J.P.: Phase suppression in the transient stages of interdiffusion in thin films, *Thin Solid Films*, **142**, 47 – 64, (1986).

[30] Benesovsky, F., Rudy, E.: Contribution to the systems zirconium-carbon and hafnium-carbon, *Planseeber. Pulvermetall.*, **8,** [2], 66 – 71, (1960).

[31] Joguet, M., Lengauer, W., Bohn, M., Bauer, J.: High-temperature reactive phase formation in the Nb-N system, *J. Alloy Comp.*, **269**, 233 – 237, (1998).

[32] P. A. Stadelmann. JEMS - EMS java version, 2004.